

Strain-dependent Dynamic Soil Properties for Wide Range of Shear Strains for North East Region

Shiv Shankar Kumar¹, Pradeep Kumar Dammala² and A. Murali Krishna³

¹Assistant Professor, Department of Civil Engineering, National Institute of Technology Patna, Bihar, India - 800005, Email: k.shiv.ce@nitp.ac.in

²Assistant Professor, Department of Civil and Infrastructure Engineering, Indian Institute of Technology Jodhpur, Rajasthan, India - 342037, Email: dammala@iitg.ac.in

³Professor, Department of Civil and Environmental Engineering, Indian Institute of Technology Tirupati, Andhra Pradesh, India - 517506, Email: amk@iittp.ac.in

Abstract. This paper presents the dynamic properties of northeast Indian river bed soil over wide strain range (0.001% to 5%) based on extensive laboratory tests. Resonant column tests data and cyclic triaxial apparatuses have been utilized to obtain the required soil parameters along with the liquefaction potential of the soil at different testing conditions. A new correlation has been proposed to find out maximum shear modulus at very low shear strain (~10-4%). The obtained results were compared with the existing literatures, which shows the importance of site-specific dynamic soil properties. Furthermore, the variations of excess pore water pressure, based on cyclic loading, reflects the soil liquefaction which can be further utilized in ground response studies for the evaluation of earthquake resist design parameters.

Keywords: Dynamic properties, low shear strains, high shear strains, resonant column tests, cyclic triaxial tests, liquefaction potential.

1 Introduction

The Northeastern India, located close to the Himalayan seismic belt, experience moderate (moment magnitude, $M_w \leq 6.0$) to large earthquakes ($6.0 < M_w \leq 8.0$) very often. This region also has witnessed two great earthquakes ($M_w > 8.0$) one each in 19th and 20th centuries (Kayal, 2012), see Fig. 1. The past seismic events also lead to wide spread liquefaction in this region especially during 1897 Shillong earthquake and 1950 Assam earthquake (Oldham, 1899; Raghu Kanth, 2010). Researchers predict that this region is due to a large impounding earthquake in the near future (Khattri, 1992).

Figure 1 presents the tectonic setup map of Northeast India superposed with seismic events ($M_w \geq 6.0$) since 1897. As it is impossible to predict, warn or prevent the occurrence of these natural calamities, the way forward in reducing the impact is through better preparedness by having efficient aseismic design of infrastructure especially for lifeline structures like bridges, dams, etc. Some of these structures were built much before the seismic codal developments in India and hence, researchers have initiated requalification studies of such structures (Dammala et al., 2017a; Krishna et al., 2014;

Sarkar et al., 2014). Seismic design of any structures require the dynamic characteristics (modulus degradation and damping variation) of underlying soil in order to incorporate the soil structure interaction effects, and such dynamic behaviour is different for different soils. It is very well recognised that underlying soil plays a crucial role in evaluating the stability of the overlying structure. But, due to unavailability of the site-specific or region-specific dynamic soil properties, geotechnical engineers are forced to use existing dynamic properties curves, which has been developed for other regions.

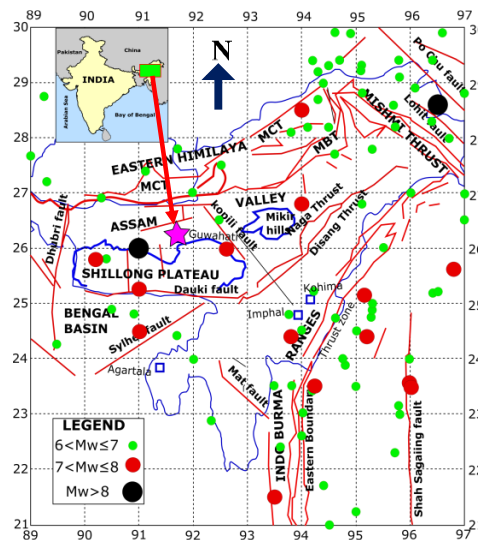


Fig. 1. Seismotectonic map of Northeast India (after Raghu Kanth, 2010)

The response of soil to each earthquake is unique depending upon strength and stiffness properties of the soil and also on the parameters of exciting motion. Some earthquakes can induce very small strains in the soil, while some could trigger significant strains which can mobilize the entire shear strength of soil. Hence, the strength of soil with varying strains (shear modulus, G and Damping ratio, D) is required to perform an aseismic design of structures. Researchers have proposed such strain dependant dynamic soil properties based on extensive experimental and analytical relationships (Seed and Idriss, 1970; Vucetic and Dobry, 1991; Ishibashi and Zhang, 1993; Darendali, 2001; Vardanega and Bolton, 2013). Based on these observations, the main objective of article is to obtain the strength and stiffness of the soil of this highly active seismic region. The dynamic characterization of chosen sand was obtained using soil element testing techniques such as Resonant column (RC) and Cyclic Triaxial (CTX) at different loading conditions (varying shear strain levels, confining pressures and initial void ratios). The results from each testing technique are presented in terms of shear modulus and damping variation with shear strain (γ) and finally combined to have the desired properties over wide strain range.

2 Experimental Program

2.1. Material

Brahmaputra Sand (BS) collected from Brahmaputra River near Guwahati region, Assam (India). The particle size distribution of the sand combined with probable liquefiable zones for sandy soils is shown in Fig. 2, which confirms that BS is highly susceptible to liquefaction. Index properties of the soil were determined according to the ASTM standards and are presented in Table 1. The soil has been classified as poorly graded sand (SP) according to Unified Soil Classification System.

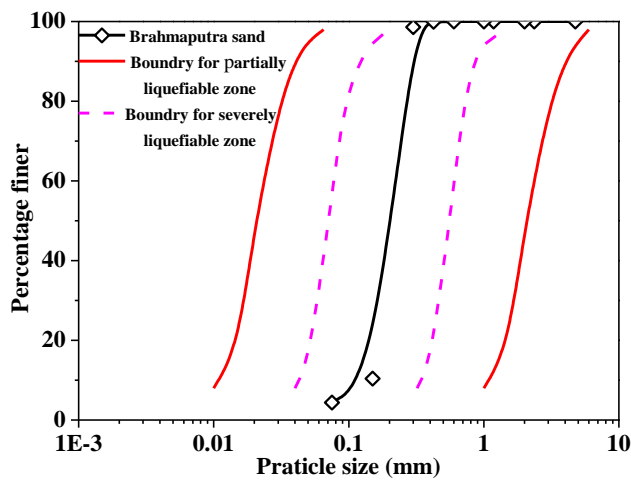


Fig. 2. Particle size distribution of BS compared with liquefiable soil zones proposed in (Xenaki and Athanasopoulos, 2003)

Table 1. Index properties of sand

Soil descriptions	values	Code followed
Mean grain size, D_{50} (mm)	0.21	(ASTM D6913)
Minimum unit wt. (kN/m^3)	13.85	(ASTM D4254)
Maximum unit wt. (kN/m^3)	16.84	(ASTM D4253)
Uniformity coefficient (C_u)	1.47	
Coefficient of curvature (C_c)	1.09	
Specific gravity	2.7	(ASTM D0854)
Classification symbol	SP	(ASTM D2487)

2.2. Sample preparation and testing procedures

In order to obtain the strain dependant dynamic soil properties (G and D), RC and CTX apparatus have been utilized as one single equipment cannot provide G and D variation over the required strain range (0.001% to 5%). RC tests can provide reliable dynamic characterization up to a shear strain level of 0.1%, while CTX tests can furnish up to a strain level of 5%. Sample preparation and testing procedure of RC and

CTX tests were followed according to the standards, ASTM D4015 and ASTM D3999, respectively and are described in detail by Dammala et al. (2017b) and Kumar et al. (2017a), respectively. Tests are aimed to predict the dynamic soil properties at varying effective confining pressures (σ'_c) and varying relative densities (D_r). The summary of the testing programme is listed in Table 2.

Table 2. Investigating parameters for RC and CTX tests

Test	D_r ($\pm 2\%$)	e	σ'_c (kPa)	Results presented	
RC	30 ($e_{target} = 0.860$)	0.865 0.851 0.854	50 100 300	G - γ , D - γ from 0.0005% to 0.1% (Dammala et al., 2017b)	
	50 ($e_{target} = 0.792$)	0.789 0.804 0.798	50 100 300		
	70 ($e_{target} = 0.724$)	0.718 0.725 0.712	50 100 300		
	30	0.856	50 to 600		Maximum shear modulus (G_{max}) and Minimum damping ratio (D_{min})
	50	0.780	50 to 600		
	70	0.717	50 to 600		
	CTX	30 ($e_{target} = 0.860$)	0.868 0.856 0.863	50 100 150	G - γ , D - γ from 0.015% to 4.5% (at 10 different strain levels) and liquefaction evaluation (Kumar et al., 2017a)
		60 ($e_{target} = 0.758$)	0.765 0.746 0.741	50 100 150	
		90 ($e_{target} = 0.656$)	0.667 0.672 0.650	50 100 150	

3 Results and Discussions

3.1. Evaluation of shear modulus (G) at small strain

The variation of shear modulus with γ for BS obtained from RC tests at different σ'_c and D_r are presented in Figs. 3a and b respectively. An increase of G with the increase of σ'_c can be observed which clearly indicates that the dynamic shear modulus increases with the overburden pressure. Figure 3b depicts that G increases with D_r and the difference diminishes as strain approaches 0.1%.

3.2. A new empirical correlations to evaluate maximum shear modulus (G_{max})

Several researchers have proposed empirical correlations to evaluate the maximum shear modulus (G_{max}) of sandy soil (Chung et al., 1984; Hardin and Richart, 1963; Saxena and Reddy, 1989). In the absence of resonant column tests data, researchers have used existing correlations to evaluate G_{max} , presented in Table 3.

Table 3 clearly indicates that each regions may have different correlations for the evaluation of G_{max} , depending upon the particle sizes. In the present study, the results obtained from RC tests are used to form an empirical correlation (Eqn. 1) for G_{max} determination.

$$G_{max} = \frac{592.25 \times (P_a)^{0.516} \times (\sigma'_c)^{0.484}}{(0.3 + 0.7e^2)} \quad (1)$$

where, σ'_c = effective confining stress (kPa); P_a = atmospheric pressure (kPa); e = void ratio. Figure 4a shows the comparison between the observed value (based on experimental results) and predicted values (based on the Eqn. 1) at different σ'_c and D_r . It can be seen that the proposed correlation provides better estimation of G_{max} for BS (with only 2-4% error). Figure 4b testifies the efficiency of Eqn. 1.

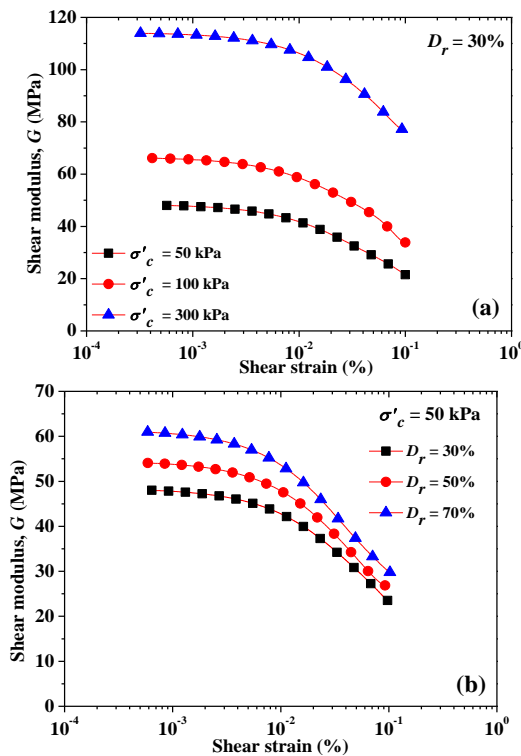


Fig. 3. Variation of shear modulus with shear strain for BS sand at different (a) σ'_c and (b) D_r (after Dammala et al., 2017b)

3.3. A new empirical correlations to evaluate small strain damping ratio

Figure 5a presents the variation of damping ratio (D) with γ at different σ'_c and D_r . It can be seen that D increases with γ , and decreases with σ'_c . Based on the regression analysis of the experimental data, an equation (Eqn. 2) for the D is developed. Similar correlations were proposed by Saxena and Reddy (1989) and Chattaraj and Sengupta (2016) for Monterey sand and Kasai sand, respectively.

$$D = 24.4 \left(\frac{\sigma'_c}{P_a} \right)^{-0.4} (\gamma)^{0.6} \quad (2)$$

The predicted D based on the Eqn. (2), depicted in Fig. 5a, shows close agreement with the experimental data.

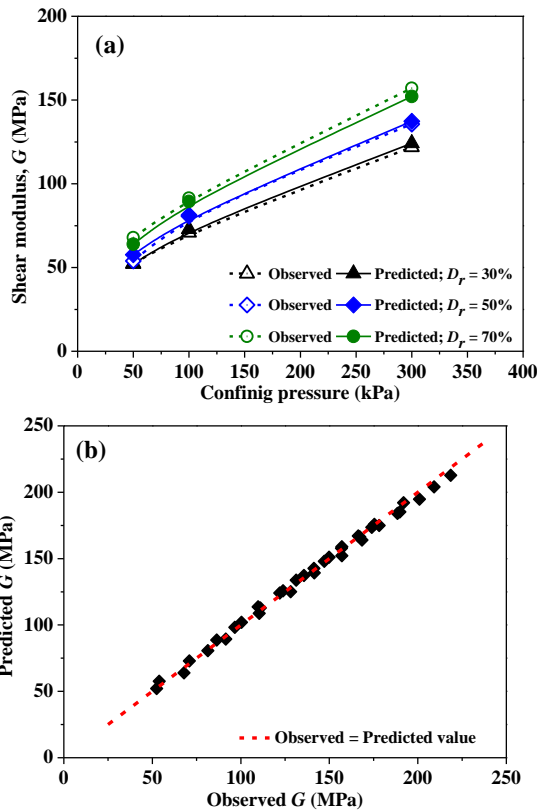


Fig. 4. (a) Observed and predicted shear modulus at different D_r and (b) Comparison of measured G_{max} from RC tests and predicted using Eqn. (1)

Figure 5b illustrates the negligible effect of D_r on damping ratio (D). It is seen that, for a constant σ'_c , the experimental and predicted data falls in narrow range. Figure 5c describes the deviation between experimentally obtained data and predicted data

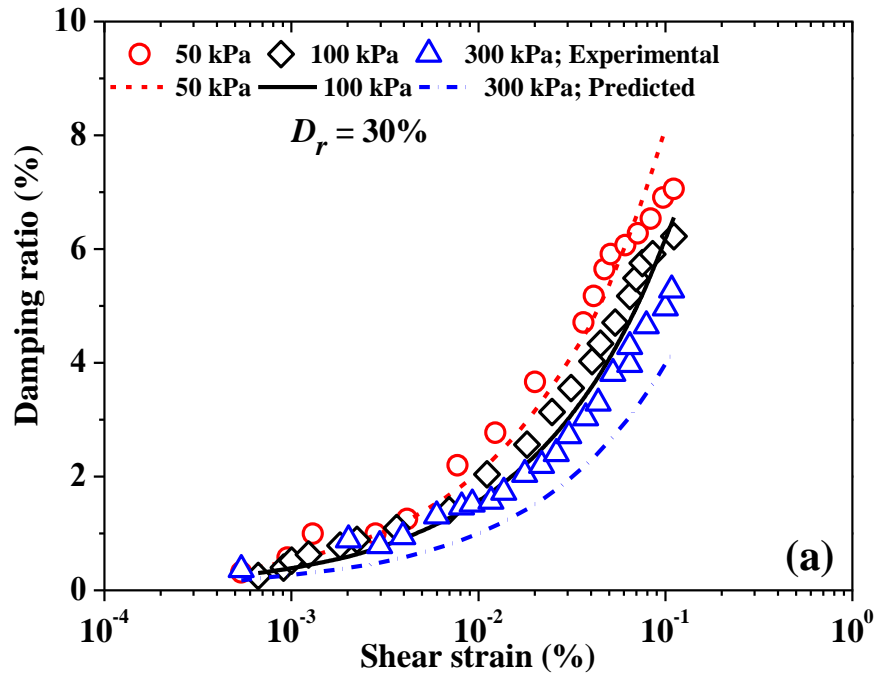
based on Eqn. (2). Figure 6a presents the variations of G/G_{max} and D with the γ at different σ'_c . It can be observed that the effect of σ'_c on the G/G_{max} curve and D -curve are negligible for low strain range ($\gamma < 0.001\%$) beyond which the effect is significant. Since, higher σ'_c impart higher resistance to deform, the G will be higher. This shows the linear elastic behaviour of soils at low strain range ($<0.001\%$) and with further shearing, plastic behaviour (permanent volume change) can be seen. Similar concept of linear elastic and plastic zones for cohesionless soils based on modulus degradation curves was explained in the literatures (Dammala et al., 2015; Hsu and Vucetic, 2004; Vucetic, 1995). It is also evident from the Fig. 6a that D decreases with σ'_c and increases with γ . Figure 6b depicts that the G/G_{max} and D with the γ at different D_r . It shows that the D_r has negligible effect on G/G_{max} and D , meaning, the compactness of the soil specimen doesn't affect the damping behaviour. Similar trends were also observed for other σ'_c , which are not presented here for brevity.

Table 3. Correlations to evaluate G_{max} for Indian and other region sand

Sands	Correlations	Reference strain	References	
Other region sandy soil	$G_{max} = 1230 \frac{(2.973 - e)^2}{(1 + e)} (\sigma'_c)^{0.5}$	$\leq 10^{-5}$	Hardin and Drnevich (1972)	
	$G_{max} = 900 \frac{(2.17 - e)^2}{(1 + e)} (\sigma'_c)^{0.4}$	$\leq 10^{-5}$	Iwasaki and Tatsuoka (1977)	
	$G_{max} = 850 \frac{(2.17 - e)^2}{(1 + e)} (\sigma'_c)^{0.44}$			
	$G_{max} = 700 \frac{(2.17 - e)^2}{(1 + e)} (\sigma'_c)^{0.5}$			
	$G_{max} = \frac{625 \times (P_a)^{0.5} \times (\sigma'_c)^{0.5}}{(0.3 + 0.7e^2)}$	$\leq 10^{-5}$	Hardin (1978)	
	Ottawa sand	$G_{max} = \frac{(32.17 - 14.8e)^2}{(1 + e)} (\sigma'_c)^{0.5}$	$\leq 10^{-5}$	Hardin and Richart (1963)
	Toyora sand	$G_{max} = 840 \frac{(2.17 - e)^2}{(1 + e)} (\sigma'_c)^{0.5}$	$\leq 10^{-5}$	Kokusho (1980)
		$G_{max} = 1230 \frac{(2.973 - e)^2}{(1 + e)} (\sigma'_c)^{0.5}$		Drnevich (1978)
	Monterey No. 0 sand	$G_{max} = \frac{523 \times (P_a)^{0.52} \times (\sigma'_c)^{0.48}}{(0.3 + 0.7e^2)}$	$\leq 10^{-5}$	Chung et al. (1984)
		$G_{max} = \frac{428.2 \times (P_a)^{0.426} \times (\sigma'_c)^{0.574}}{(0.3 + 0.7e^2)}$		Saxena and Reddy (1989)

Indian sandy soil	Ennore sand	$G_{\max} = 9280 \frac{(2.626 - e)^2}{(1 + e)} (\sigma'_c)^{0.4}$	$\leq 10^{-5}$	Mallik and Baidya (2014)
	Local sand	$G_{\max} = 7500 \frac{(2.603 - e)^2}{(1 + e)} (\sigma'_c)^{0.4}$		
	Clean sand	$G_{\max} = 102150.95 \frac{(2.973 - e)^2}{(1 + e)} (\sigma'_c)^{0.5}$	$\leq 10^{-5}$	Dutta and Saride (2014)
		$G_{\max} = 102132.65 \frac{(2.973 - e)^2}{(1 + e)} (\sigma'_c)^{0.5}$		Kumar and Achu (2014)
	Kasai sand	$G_{\max} = \frac{611.58 \times (P_a)^{0.532} \times (\sigma'_c)^{0.468}}{(0.3 + 0.7e^2)}$	$\leq 10^{-5}$	Chattaraj and Sengupta (2016)
BS	$G_{\max} = \frac{592.25 \times (P_a)^{0.516} \times (\sigma'_c)^{0.484}}{(0.3 + 0.7e^2)}$	$\approx 4 \times 10^{-4}$	Present study	

Note: G_{\max} = maximum dynamic shear modulus; e = void ratio; σ'_c = effective confining pressure; P_a = atmospheric pressure



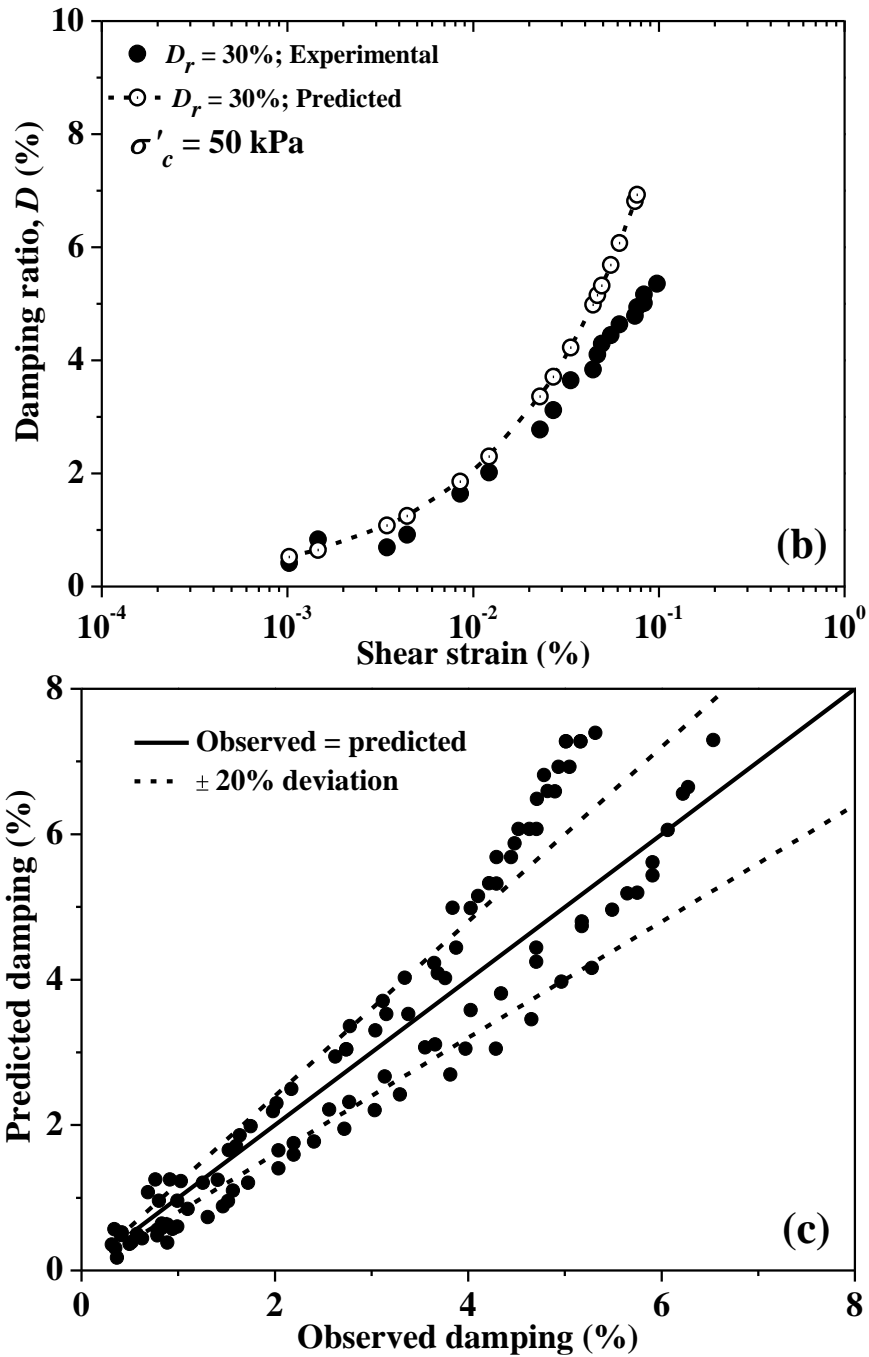


Fig. 5. Observed and predicted D at different (a) σ'_c (b) D_r (c) Comparison with the proposed

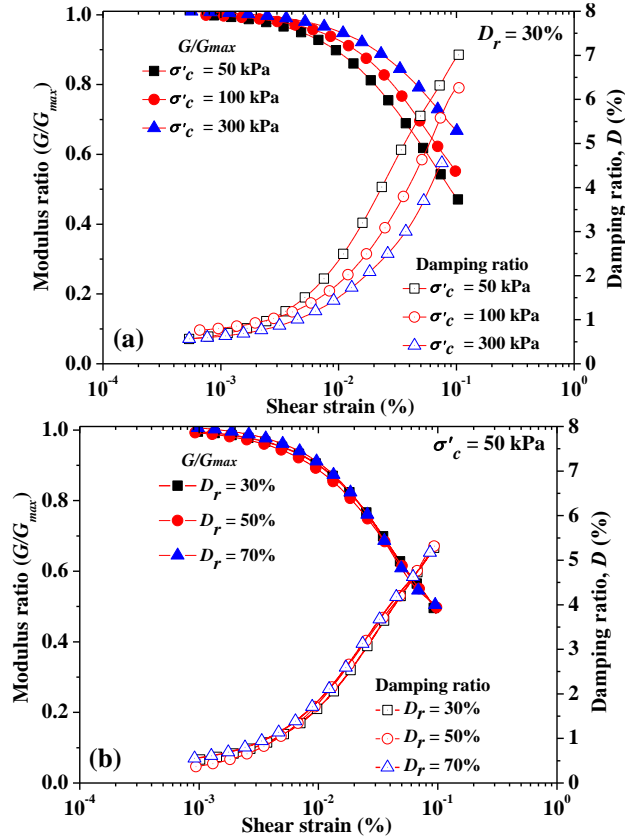


Fig. 6. Variation of G/G_{max} and D with shear strain for BS sand at different (a) σ'_c and (b) D_r (after Dammala et al., 2017b)

4 Cyclic Triaxial Tests

As RC tests provided the dynamic soil properties up to 0.1% shear strain, properties over the remaining required range (up to 5%) was obtained using CTX testing. Since, Dammala et al. (2017b) conducted the tests on dry cohesionless soil up to $\gamma = 0.1\%$, it is not practically justified to use this results of strain range 0.0001% to 0.1%, in case of saturated sand. It was reported in the literature (Vucetic and Dobry, 1988; Hashash et al., 2016; Kong et al., 2018), that the shear strain of 0.01% is a limiting value of volumetric threshold shear strain below which no significant pore water pressure is generated in the saturated cohesionless specimen. Therefore, the consideration of low-strain dynamic properties of soil up to $\gamma = 0.01\%$ will not violate the assumption that the dynamic properties of dry and saturated cohesionless soil up to 0.01% are nearly same. CTX tests have been used to evaluate the shear modulus and damping ratio of BS for high shear strain range i.e. from 0.01% to 5%. The typical stress strain behavior of a cyclically loaded soil is expected to follow the hysteresis loop and was observed to be asymmetrical (Fig. 7) at shear strains greater than 0.15% (Kumar et al.,

2017a). This high-strain (>0.01%) dynamic properties of cohesionless soil was taken from Kumar et al. (2017a).

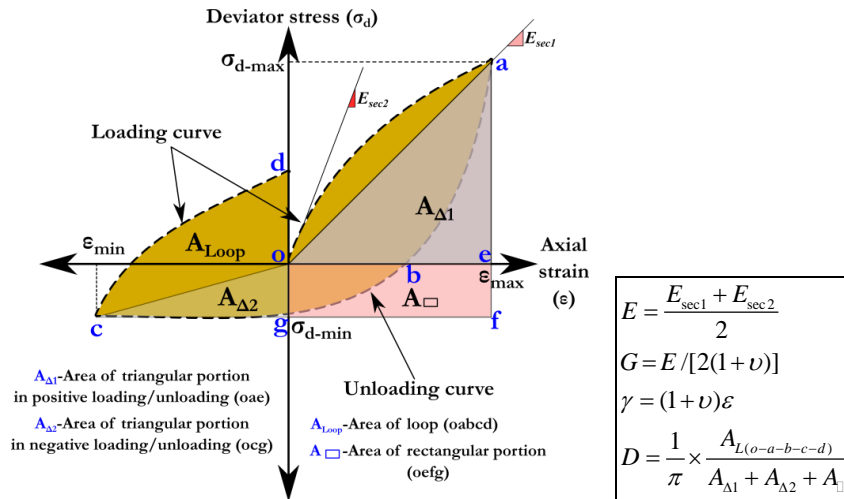


Fig. 7. A typical asymmetrical hysteresis loop (after Kumar et al., 2017a)

5 Comparison of BS Results with Other Indian Sandy Soil Data

Figure 8 presents the variations of G/G_{max} and D for wide range of γ (evaluated using both RC and CTX) at different σ'_c and D_r . Figure 8a shows the comparison of G/G_{max} of BS with G/G_{max} curves suggested in literatures such as Seed and Idriss (1970), Ishibashi and Zhang (1993) and Darendali (2001). Seed and Idriss (1970) provided broad range of G/G_{max} curve for sand, which is commonly used in GRA due to the lack of site-specific data (Chatterjee and Choudhury, 2016; Kumar et al., 2017b; Kumar et al., 2018). It can be clearly seen that RC and CT data of BS soil does not fall in range proposed by Ishibashi and Zhang (1993) and Seed and Idriss (1970) while consistent with Darendali (2001) curves at high strains. Figure 8b describes the variation of D of BS obtained from RC and CT tests, and, compared with the above discussed traditional curves. It can be seen that both RC and CTX data up to $\gamma = 1\%$, falls in the lower range of Seed and Idriss (1970) curve beyond which D decreases. It can also be observed from Fig. 8b, that the Ishibashi and Zhang (1993) shows significantly higher damping than the estimated damping values, whereas Darendali (2001) shows the lower values of damping at shear strains greater than 0.2%.

Figure 9 present the variations of G/G_{max} (Fig. 9a) and damping (Fig. 9b) with shear strain for sands of Indian region. The data other than BS soil was taken from the mentioned literatures in Fig. 9. A range in terms of lower and upper bound is provided for G/G_{max} curve in which all Indian sands accommodate. This upper and lower bounds of G/G_{max} and D of Indian sands can be useful for the many site-specific engineering applications such as seismic GRA.

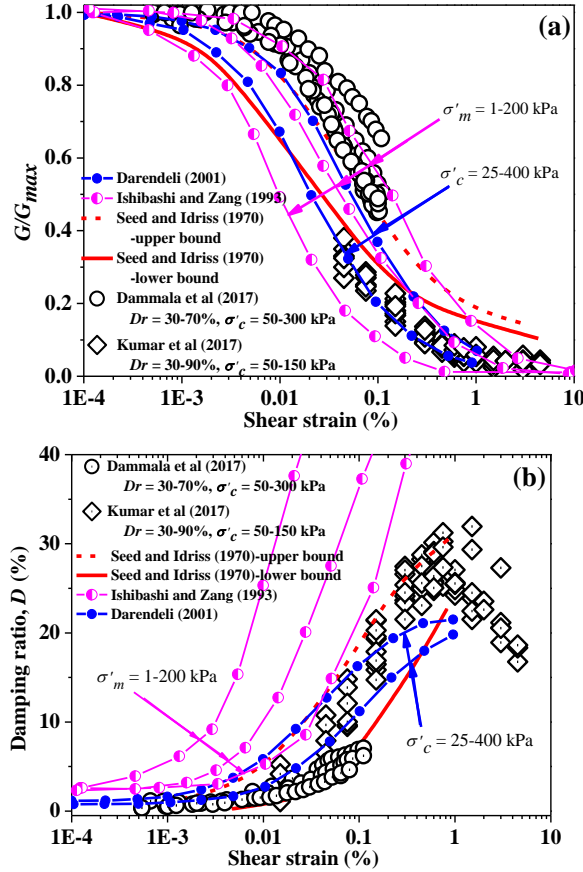


Fig. 8. Variations of (a) G/G_{max} and (b) D curve with shear strain from RC and CT tests at different σ'_c and D_r .

6 Conclusions

In this study, resonant column and cyclic triaxial tests data at different testing conditions are presented to characterize the dynamic behavior of BS soil. Resonant column tests were conducted at low strain level whereas, cyclic triaxial tests at higher shear strain and the following conclusions were drawn:

1. Based on the resonant column tests, a new correlation has been proposed to find out maximum shear modulus of BS at very low shear strain ($\sim 10^{-4}\%$).
2. Shear modulus degradation and damping ratio for wide range of shear strain i.e. from $10^{-4}\%$ to 5% has been compared with existing material models, which emphasize the importance of site-specific dynamic properties of Indian sandy soil.
3. PWP variation in cyclic triaxial reflects that the r_u decreases with the increase of D_r , means at higher D_r , higher N_c are required to liquefy the soil specimens for acon-

stant γ and σ'_c . The r_u significantly decreases with the increase of σ'_c whereas, the same is marginally affected, which can be neglected, by D_r for first loading cycles.

Therefore, the obtained wide strain range dynamic soil properties combined with PWP parameters will be highly useful in performing non-linear effective stress GRA studies in Northeast India.

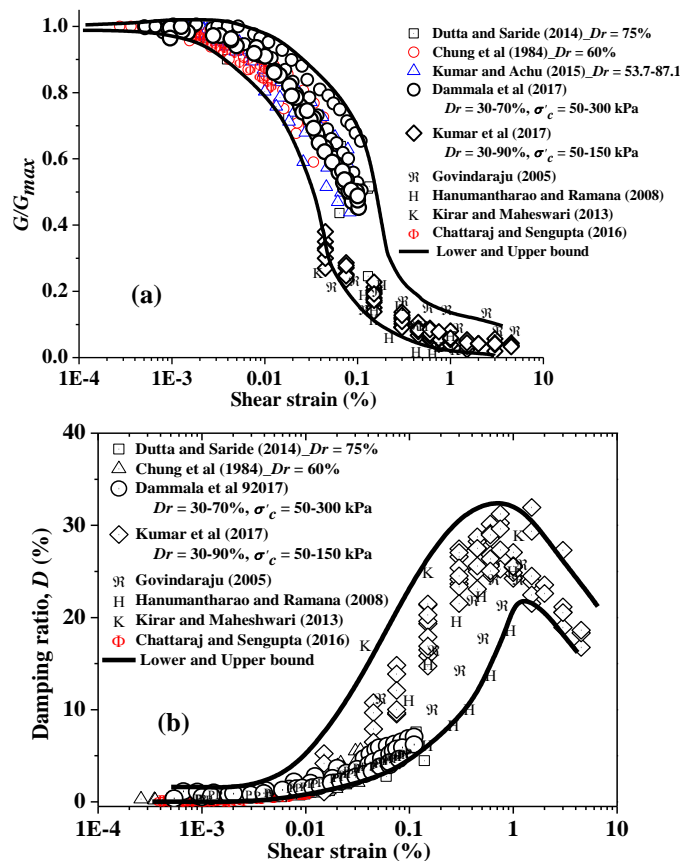


Fig. 9. Variations of (a) G/G_{max} and (b) Damping with shear strain for Indian sandy soils

References

1. ASTM, Standard D0854: Standard test methods for specific gravity of soil solids by water pycnometer. *ASTM International*, West Conshohocken, PA (2014).
2. ASTM D6913/D6913M: Standard test methods for particle-size distribution (gradation) of soils using sieve analysis. *ASTM International*, West Conshohocken, PA (2017).

3. ASTM D4254: Standard test methods for minimum index density and unit weight of soils and calculation of relative density. *ASTM International*, West Conshohocken, PA (2016).
4. ASTM D4253: Standard test methods for maximum index density and unit weight of soils using a vibratory table. *ASTM International*, West Conshohocken, PA (2016).
5. ASTM D4015: Standard test methods for modulus and damping of soils by resonant-column. *ASTM International*, West Conshohocken, PA (2007).
6. ASTM D3999/D3999M: Standard test methods for the determination of the modulus and damping properties of soils using the cyclic triaxial apparatus. *ASTM International*, West Conshohocken, PA (2011).
7. ASTM D2487: Standard practice for classification of soils for engineering purposes (Unified Soil Classification System). *ASTM International*, West Conshohocken, PA (2011).
8. Chattaraj, R., Sengupta, A.: Liquefaction potential and strain dependent dynamic properties of Kasai River sand. *Soil Dynamics and Earthquake Engineering*, 90, 467–475, (2016).
9. Chatterjee, K., Choudhury, D.: Influences of local soil conditions for ground response in Kolkata city during earthquakes. In Proceedings of the National Academy of Sciences, India Section A: Physical Sciences, 1-14, (2016).
10. Chung, R. M., Yokel, F. Y., Dmievich, V. P.; Evaluation of dynamic properties of sands by resonant column testing. *Geotechnical Testing Journal*, 7, 60-69, (1984).
11. Dammala, P. K., Bhattacharya, S., Krishna, A. M., Kumar, S. S., Dasgupta, K.: Scenario based seismic re-qualification of caisson supported major bridges - A case study of Saraighat Bridge. *Soil Dynamics and Earthquake Engineering*, 100, 270–275, (2017a).
12. Dammala, P. K., Murali Krishna, A., Bhattacharya, S.: Cyclic threshold shear strains in cohesionless soils based on stiffness degradation. In Proceeding of Indian Geotechnical Conference, Pune, Maharashtra, India, (2015).
13. Dammala, P. K., Murali Krishna, A., Bhattacharya, S., Nikitas, G., Rouholamin, M.: Dynamic soil properties for seismic ground response studies in Northeastern India. *Soil Dynamics and Earthquake Engineering*, 100, 357–370, (2017b).
14. Darendeli, M.: Development of a new family of normalized modulus reduction and material damping. *University of Texas*, (2001).
15. Dmievich, V.P.: Draft report of the initial ASTM resonant column round robin testing program. University of Kentucky, Lexington, KY, pp.20, (1978).
16. Dobry, R., Abdoun, T.: Cyclic shear strain needed for liquefaction triggering and assessment of overburden pressure factor $K\sigma$. *Journal of Geotechnical and Geoenvironmental Engineering*, 141, 1–18, (2015).
17. Dobry, R., Ladd, R., Yokel, F., Chung, R., Powell, D.: Prediction of pore water pressure buildup and liquefaction of sand during earthquakes by the cyclic strain method. pp. 138, Gaithersburg, MD: *National Bureau of Standards*, (1982).
18. Dutta, T. T., Saride, S.: Dynamic properties of clean sand from resonant column. In Proceeding of Indian Geotechnical Conference, Kakinada, India, (2014).
19. Govindaraju, L.: Liquefaction and dynamic properties of sandy soils. *PhD Thesis*, Submitted to Indian Institute of Science Bangalore, (2005).

Proceedings of Indian Geotechnical Conference 2020
December 17-19, 2020, Andhra University, Visakhapatnam

20. HanumanthaRao, C., Ramana, G. V.: Dynamic soil properties for microzonation of Delhi. *Journal of Earth System and Science*, 117, 719–730, (2008).
21. Hardin, B. O., Drenvich, V. P.: Shear modulus and damping in soils: design equations and curves. *Journal of Soil Mechanics and Foundation Divison*, 7, 667–692, (1972).
22. Hardin, B. O., Richart, F. E.: Elastic wave velocities in granular soils. *Journal of Soil Mechanics and Foundation Divison*, 89, 33–65, (1963).
23. Hardin, B.O.: The nature of stress-strain behaviour for soils. In Proceeding of Earthquake Engineering, *Soil Dynamics Pasadena, CA: ASCE*, 1, 3-90, (1978).
24. Hashash, Y. M. A., Musgrove, M. I., Harmon, J. A., Groholski, D. R., Phillips, C., Park, D.: DEEPSOIL 6.1. User Manual, (2016).
25. Hsu, C. C., Vucetic, M.: Volumetric Threshold shear strain for cyclic settlement. *Journal of Geotechnical and Geoenvironmental Engineering*, 130, 58–70, (2014).
26. Ishibashi, I., Zhang, X.: Unified dynamic shear moduli and damping ratios of sand and clay. *Soils and Foundations*, 33, 182–191, (1993).
27. Iwasaki, T., Tatsuoka, F.: Effect of grain size and grading on the dynamic shear moduli of soils. *Soils and Foundations*, 17, 19-35, (1977).
28. Kayal, J. R., Arefiev, S. S., Baruah, S., Hazarika, D., Gogoi, N., Gautam, J. L., Baruah, S., Dorbath, C., Tatevossian, R.: Large and great earthquakes in the Shillong plateau–Assam valley area of Northeast India Region: Pop-up and transverse tectonics. *Tectonophysics*, 532, 186-192, (2012).
29. Khattri, K. N.: Probabilities of occurrence of great earthquakes in the Himalaya, In Proceedings of the Indian Academy of Sciences-Earth and Planetary Sciences. 108, 87–92, (1992).
30. Kirar, B., Maheswari, B.: Effects of silt content on dynamic properties of solani sand. In Proceeding of 7th International Conference on Case History in Geotechnical Engineering, pp. 1–7, (2013).
31. Kokusho, T.: Cyclic triaxial test of dynamic soil properties for wide strain range. *Soils and Foundations*, 20, 45-60, (1980).
32. Kong, G., Li, H., Yang, G., Cao, Z.: Investigation on shear modulus and damping ratio of transparent soils with different pore fluids. *Granular Matter*, 20, p.8, (2018).
33. Kumar, J., Achu, C. C.: Effect of cyclic strain history on shear modulus of dry sand using resonant column tests. *Geotechnical Engineering Journal of SEAGS, AGSSEA*, 46, 99–104, (2014).
34. Kumar, S. S., Dey, A., Krishna, A. M.: Importance of site-specific dynamic soil properties for seismic ground response studies. *International Journal of Geotechnical and Earthquake Engineering*, 9, 78-98, (2018).
35. Kumar, S. S., Krishna, A. M., Dey, A.: Evaluation of dynamic properties of sandy soil at high cyclic strains. *Soil Dynamics and Earthquake Engineering*, 99, 157–167, (2017c).
36. Mallick, A., Baidya, D. K.; Parametric study of dynamic properties of cohesionless soils by resonant column tests. In Proceeding of Indian Geotechnical Conference, Kakinada, India, (2014).
37. Murali Krishna, A., Bhattacharya, S., Choudhury, D.: Seismic requalification of geotechnical structures. *Indian Geotechnical Journal*, 44, 113-118, (2014).

Shiv Shankar Kumar, Pradeep Kumar Dammala and A. Murali Krishna

38. Oldham, R. D.: Report of the great earthquake of 12th June, 1897, Office of the Geological survey, (1899).
39. Raghu Kanth, S. T. G., Dash, S. K.: Evaluation of seismic soil-liquefaction at Guwahati city. *Environmental Earth Science*, 61, 355–368, (2010).
40. Sarkar, R., Bhattacharya, S., Maheshwari, B. K.: Seismic requalification of pile foundations in liquefiable soils. *Indian Geotechnical Journal*, 44, 183-195, (2014).
41. Saxena, S. K., Reddy, K. R., Dynamic moduli and damping ratios for Monterey No.0 sand by resonant column tests. *Soils and Foundations*, 29, 37–51, (1989).
42. Seed, H. B., Idriss, I. M.: Soil moduli and damping factors for dynamic response analysis. *Report EERC*, 70, p. 10, (1970).
43. Vardanega, P. J., Bolton, M. D.: Stiffness of clays and silts: Normalizing shear modulus and shear strain. *Journal of Geotechnical and Geoenvironmental Engineering*, 139, 1575-1589, (2013).
44. Vucetic, M.: Cyclic Threshold Shear strains in soils. *Journal of Geotechnical and Geoenvironmental Engineering*, 120, 2208–2228, (1995).
45. Vucetic, M.: Pore pressure buildup and liquefaction at level sandy sites during earthquakes. *Rensselaer Polytechnic Institute*, Troy, NY, (1986).
46. Vucetic, M., Dobry, R.: Cyclic triaxial strain-controlled testing of liquefiable sands. In *Advance Triaxial Test of Soil and Rock*, pp. 475–485, (1988).
47. Vucetic, M., Dobry, R.: Effect of soil plasticity on cyclic response. *Journal of Geotechnical Engineering*, 117, 89-107, (1991).
48. Xenaki, V. C., Athanasopoulos, G. A.: Liquefaction resistance of sand-mixtures: an experimental investigation of the effect of fines. *Soil Dynamics and Earthquake Engineering*, 23, 183-194, (2003).